A Suggested Technique for the Analysis of Airborne Continuous Ice Nucleus Data

JAMES A. HEIMBACH, JR.

Department of Earth Sciences, Montana State University, Bozeman 59715

ARLIN B. SUPER AND JOHN T. MCPARTLAND

Division of Atmospheric Water Resources Management, U. S. Bureau of Reclamation, Miles City, Mont. 59301

(Manuscript received 6 August 1976, in revised form 22 February 1977)

ABSTRACT

The problem of reducing data from continuously recording ice nucleus counters is addressed. These instruments characteristically have large response times which make their data difficult to interpret. A statistical theory of instrument response is developed which parameterizes the response of these instruments and reconstructs an estimate of the true count-versus-time profiles. Data from two NCAR ice nucleus counters used on separate field projects are summarized to provide example response characteristics. Field calibration techniques for these NCAR counters are also described. Although intended for use on ice nucleus counters, the interpretation techniques are applicable to other continuously recording instruments having significant response times.

1. Introduction

With the increasing concern for the targeting effectiveness of both ground-based and aerial releases of ice nucleating agents (see, e.g., Rottner *et al.*, 1975), the need for airborne tracing is being realized. There are at least two devices which detect these submicroscopic particles on a continuous, near real-time basis. These are the NCAR counter described by Langer *et al.* (1967) and Langer (1973), which acoustically detects ice crystals, and the commercially available Mee unit, which uses an optical detection scheme suggested by Fukuta and Kramer (1968) and Turner and Radke (1973). Both of the above detect ice crystals grown about ice nuclei in an artificial, supercooled cloud which induces considerable smoothing and lag times. This is not critical for static sampling; however, with airborne tracing the count data can be easily misinterpreted as to both location and true ambient count. The high speed of the sampling platform and the large lag and smoothing times involved combine to give counts lower than reality for thin plumes and distance errors in the range of kilometers.

In the sections which follow, the theoretical and practical techniques are outlined to interpret data having a lag in response and a large degree of smoothing. Section 2 describes two NCAR ice nucleus counters which were used to obtain the example response characteristics delineated in Section 4. In Section 3 the theory for parameterizing the response of an instrument of this type is developed, and suggestions for its operational applications are given in Section 5.

2. Instrumentation and data collection

The data which were used to provide example response characteristics came from two NCAR ice nucleus counters used on two separate projects. The concepts, though not the parameters, can be applied to other designs of counters. The intention of both projects was to use silver iodide (AgI) in plume-tracing experiments. One was a diffusion study conducted at Colstrip, Mont., and the other was a test of the effectiveness of hail storm treatment in Alberta, Canada, using ground releases of AgI. The Montana instrument (hereafter "Unit A") was specifically built for airborne use. It was more compact overall and had a smaller cloud chamber than the more common laboratory unit. Table 1 describes the specifics of this unit. Its field application is described by Super (1974) and Super *et al.* (1975). During the summer of 1975 there was an opportunity to examine the characteristics of another NCAR counter ("Unit B") which belonged to the Alberta Research Council and which was being used on a ground-based plume study conducted in cooperation with the Alberta Hail Suppression Project. This unit was bulkier and had a larger cloud chamber than the former. Two vacuums are listed in Table 1 for this unit because, during part

TABLE 1. Specifications of the two NCAR ice nucleus counters applied. (Unit A is from BUREC and Unit B was loaned by the Alberta Research Council.)

	Unit A	Unit B
Construction	E. Bolay Assoc., modified at NCAR and MSU.	E. Bolay Assoc., modified in the field by Krick Assoc.
Cloud chamber depth (cone included)	83 cm	118 cm
Cloud chamber width	18 cm	20 cm
Power	110 V ac	110 V ac
Refrigeration	Freon/compressor	Freon/compressor
Vacuum	120 mm Hg	105 and 120 mm Hg
Electronics	Linear pulse averaging circuit with five scales X1 through X10,000.	E. Bolay Assoc. Model A90000-2. Digital incrementation over time spans of 120, 12, 12 and 1.2 s corresponding to X10 through X10,000 for four scales, respectively.
Recording	Single channel Rustrack.	Rustrack with two channels.
Ice nucleus source	$AgI-NH_4I$-acetone. 2×10^{16} nuclei per gm AgI (effective at $-20°C$) 0.5 gm AgI min^{-1}.	Coke impregnated with AgI. 2×10^{14} to 10^{15} nuclei per gm AgI (effective at $-20°C$) 0.47 gm AgI min^{-1}.
Data digitizing interval	7.5 s	12 s

of the study, there was insufficient vacuum supplied by the aircraft to reach the optimal 120 mm Hg.

Ground testing of both units was done using a large hypodermic needle containing samples of AgI smoke taken from the same type of generator used in the respective ongoing field work. Unit A used the Skyfire type system burning an $AgI-NH_4I$ complex in acetone (Super *et al.*, 1972) and Unit B used the Krick Type 15 coke-fueled source. In both cases the generators were far removed downwind of the counters to minimize contamination. (However, this still occurred at times.) A plastic jar was held above the flames to collect samples. A diluted sample was drawn into a hypodermic needle and each test consisted of a timed input into the counter's inlet. Unit A was bench-tested, and Unit B had its calibration data taken while on the ground in the aircraft.

There were three basic types of sample input: an instantaneous "puff," a constant input or "box," and a series of box inputs which, if smoothed, would approximate the appearance of a normal distribution. The reason for specifying the nature of the input was to enable the variance of the input to be known, a necessary parameter when stratifying the response variance. Times of start and stop of input, times to first perceptible rise above background count and times to peak were noted. To insure later applicability to data taken during the field projects, data were digitized from the Rustrack recording over the same interval, i.e., 7.5 and 12 s, respectively. There was no attempt to integrate over the intervals; rather, instantaneous values were extracted. In the case of Unit B the counts were already integrated and the traces were a series of straight lines except for the highest scale where the 1.2 s digitizing interval gave the trace a continuous appearance.

3. Parameterizing response characteristics

There are two basic questions which are addressed: what is the lag time of the counter to an input and to what degree has the true plume profile been smoothed by the electronics and sample processing time. The former can be handled in a straightforward fashion and is broken down into three subheadings: time to register the mode count, time to register the median count and time to first response to a count above background. The latter reduces to defining the variance which is induced by the counter and added to the true time (distance)-count profile. Fig. 1 diagrams these parameters.

a. *Machine-induced variance*

The statistical model applied to the response of an ice nucleus counter assumes that the instrument can have the variance induced by its time averaging effects accurately determined. This variance, which is in units of time, can then be subtracted from the total variance indicated on the recording device to give an estimate of the true plume spread. Conversions to units of length can be done using the ground speed of the aircraft.

For one pass through the plume, each ice nucleus is assumed to be located along the cross-plume path y as a function of three variables. These are the mean position $\bar{y}$ of all nuclei, a true spread k along the flight path about $\bar{y}$, and a false spread ϵ due to the smoothing induced by the counter, i.e.,

$$y=\bar{y}+k+\epsilon. \quad (1)$$

Eq. (1) is the basic model of this analysis and does not imply anything about the shapes of the k and ϵ distributions.

If the coordinate system is displaced to have the fiducial point at $\bar{y}$, then $\bar{y}=0$, simplifying the procedures. Discrete notation will be used in the develop-

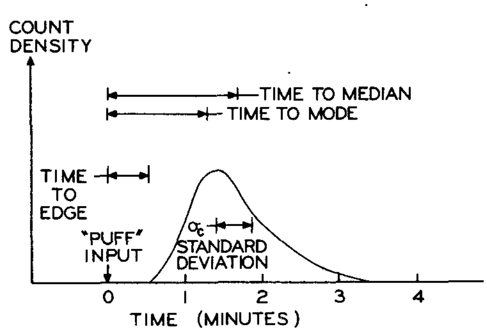

FIG. 1. Diagram of approximate response parameters.

ment because individual ice nuclei are counted, not a continuous sample as with gas sampling. Each indicated count can be considered a non-normalized, discrete density function for the point y_i, and the total or indicated variance σ_c^2 in units of length or time squared is

$$\sigma_c^2=\sum_{i=1}^{I} C_i y_i^2/N, \tag{2}$$

where

$$N=\sum_{i=1}^{N} C_i$$

is the total number of counts. Substitution of the two sources of variance for y necessitates the use of another index to account for the spread of counts about y_i. The size of this new index is a function of the position index i having the magnitude of the count at that point:

$$\sigma_c^2=\sum_{i=1}^{I}\sum_{j=1}^{C_i} (k_i+\epsilon_{ij})^2/N. \tag{3}$$

Carrying out the squaring we have

$$\sigma_c^2=\sum_{i=1}^{I}\sum_{j=1}^{C_i} (k_i^2+2k_i\epsilon_{ij}+\epsilon_{ij}^2)/N=\sum_{i=1}^{I}\sum_{j=1}^{C_i} k_i^2/N$$

$$+2\sum_{i=1}^{I}\sum_{j=1}^{C_i} k_i\epsilon_{ij}/N+\sum_{i=1}^{I}\sum_{j=1}^{C_i} \epsilon_{ij}^2/N$$

$$=\sigma_y^2+2\ \text{covariance}+\sigma_f^2. \tag{4}$$

The actual dimension of the plume transaction is parameterized in σy^2. The false or instrument-induced variance is σ_f^2. The covariance term represents the expected value of the lateral position of an ice nucleus times the displacement cause by the counter (k_i times ϵ_{ij}). One can assume that these quantities are independent if the average cloud chamber residence time, fallout rate and rate of ice crystal growth are not a function of ice nucleus concentration (and therefore lateral position y). Moreover, one must assume that the counts reported by the electronics are the same as those detected by the sensor. This last assumption may not be entirely valid for very high counts (>1000 min^{-1}) since there is a finite detection interval required which could allow several nuclei to be reported as one. Independence of the k_i and ϵ_{ij} terms allows the covariance term to be ignored (Sokal and Rohlf, 1969), giving

$$\sigma_y^2=\sigma_c^2-\sigma_f^2. \tag{5}$$

For the sake of convenience, the units of (5) will be time squared.

b. Known input variances

The problem is now reduced to estimating the machine-induced variance σ_f^2. For an instantaneous input or "puff" (actually, approximately $\frac{1}{2}$ s), σ_y is zero giving $\sigma_f^2=\sigma_c^2$. For the square input (see Fig. 2a), the variance is equal to the square of the width divided by 12. The σ_y^2 from a stepwise configuration of I box inputs (see Fig. 2b) is somewhat more complicated, and moment generating theory is used in treating this type of input (Mood and Graybill, 1963) to give

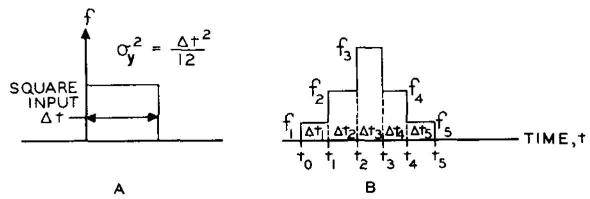

FIG. 2. Diagrams of known variance input schemes to ice nucleus counter. (Count densities $=f$.)

$$\sigma_y^2=1/(3I)\sum_{i=1}^{I} (t_i^3-t_{i-1}^3)/\Delta t_i$$

$$-[1/(2I)\sum_{i=1}^{I} (t_i^2-t_{i-1}^2)/\Delta t_i]^2$$

$$=\tfrac{1}{3}\sum_{i=1}^{I} (t_i^3-t_{i-1}^3)f_i-[\tfrac{1}{2}\sum_{i=1}^{I} (t_i^2-t_{i-1}^2)f_i]^2. \tag{6}$$

The density functions f_i are defined as

$$f_i=1/(I\Delta t_i), \tag{7}$$

giving a value inversely proportional to the rate of input from a syringe, assumed to have homogeneous contents. This satisfies the requirement that

$$\int_{-\infty}^{\infty} f(t)dt=1. \tag{8}$$

Eqs. (6) and (7) can be applied to the puff and box input cases where $I=1$ and/or $\Delta t_i=0$ to obtain the same σ_y's as outlined previously.

4. Characteristics of response

a. Calibration of raw counts

The first stage in the analysis of ice nucleus data is the conversion of recorded signals to counts per liter. The methodology to do this consists of several steps where the electronics, method of recording, ice crystal settling, deposition on walls and flow rate provide their respective contributions. Although each unit will have its own calibration, Tables 2 and 3 are shown as examples of the stages involved. In the case of Unit B, a fair amount of compensation was involved to account for the truncation imposed on the upper two scales in the digitizing process. This resulted from an additional 10:1 incrementing register placed before the recording register which tallied up to 20 counts.

TABLE 2. Stages in calibrating raw counts from unit A (x=raw signal, y=processed count in liters^{-1}).

Scale	1	10	100	1000	10,000
Analog equivalent one count min^{-1} (mA)	$A=1$	$A=0.1$	$A=0.01$	$A=0.001$	$A=0.0001$
Flow correction	1/(8.3 liters min^{-1})	—	—	—	—
Settling out factor*	10	—	—	—	—
Final calibration equation	$y=10x/8.3A$	—	—	—	—

* See Langer (1973).

Counts stored in the former register were ignored or truncated during the recording process.

b. *Scale shifts*

For the two units tested, a shift in scale would clear the integrating circuit or accumulators having the effect of starting from zero for the new scale. At such times it is appropriate to interpolate in order to smooth in the missing data. For Unit B the interpolation is a simple process of using the adjoining records; however, for Unit A, there is an interval of time needed for the response of the electronics to stabilize. This time is not necessarily longer than for the digital electronics but must be determined objectively. Fig. 3 outlines a suggested interpolation scheme for this type of electronics.

c. *Parameterization of response*

Fig. 4 shows examples of various input forms and the resulting time vs calibrated counts. Prior to drawing these, an estimate of background which equaled the minimum running mean of three intervals was subtracted from all values. Since vacuums of 105 and 120 mm were used in the field for Unit B, examples of both are shown. The response is long and variable due to the time necessary to grow ice crystals sufficiently large for detection (>20 μm) and the modes of recording. In addition, turbulence, as evidenced by the swirling segments of the cloud within the chamber, yields variable responses as packets containing differing densities of nuclei are brought to the outlet in a randomized basis. This could be at least part of the reason for the peculiar response shown in Fig. 4f.

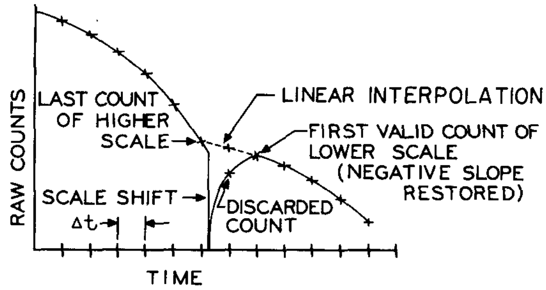

FIG. 3. Suggested interpolation scheme for estimating data lost during scale shifts for integrating electronics.

TABLE 3. Stages in calibrating raw counts from Unit B (x=raw signal, y=processed count in liters^{-1}).

Scale	10	100	1000	10 000
Registering interval (min)	$\Delta t=2.0$	$\Delta t=0.2$	$\Delta t=0.2$	$\Delta t=0.02$
Analog equivalent 1 count min^{-1} (mA)	$A=0.05$	$A=0.05$	$A=0.005$*	$A=0.005$*
Detected counts to registered counts	1:1	1:1	$\geqslant$10:1	$\geqslant$10:1
Maximum truncation error	0	0	45	450
Flow correction**	Flow (liters min^{-1}) =6.52+0.0548 ×vacuum (mm Hg) −8.63×10^{-5}×vacuum^2			
Settling out factor	10	—	—	—
Average truncation compensation	None	None	$x=x+0.0225$	$x=x+0.0225$
Final calibration equation	$y=10x/A\Delta t$ (flow)			

* Recorded as truncated to nearest 0.05 mA.
** Each sensor will have its own calibration curve.

The times to first significant rise above background ("edge time"), mode and median are listed in Table 4. Only instantaneous or "puff" input schemes were used in determining parameters other than the variances. Because of the long time intervals of accumulation for the digital electronics of Unit B, edge times were sampled using a stop watch instead of reading intervals off the strip chart. The electronics of Unit A provided a recording which allowed a precise estimate of the first rise above background. The lag of Unit A was significantly shorter than Unit B because of Unit A's smaller cloud chamber.

d. *Instrument-induced variance*

The response to a brief input bears a resemblance to a Poisson distribution which defines the expected density of a number of "rare events." For the counter

TABLE 4. Lag times (s) of edges, modes and medians. (Only "puff" type input considered.)

	Unit A	Unit B (105 mm vacuum)	Unit B (120 mm vacuum)
Number of samples	16	14	24
Time to edge	25	38	35
Standard deviation	7	8	6
Time to mode	61	77	70
Standard deviation	17	10	12
Time to median	74	102	97
Standard deviation	13	8	15

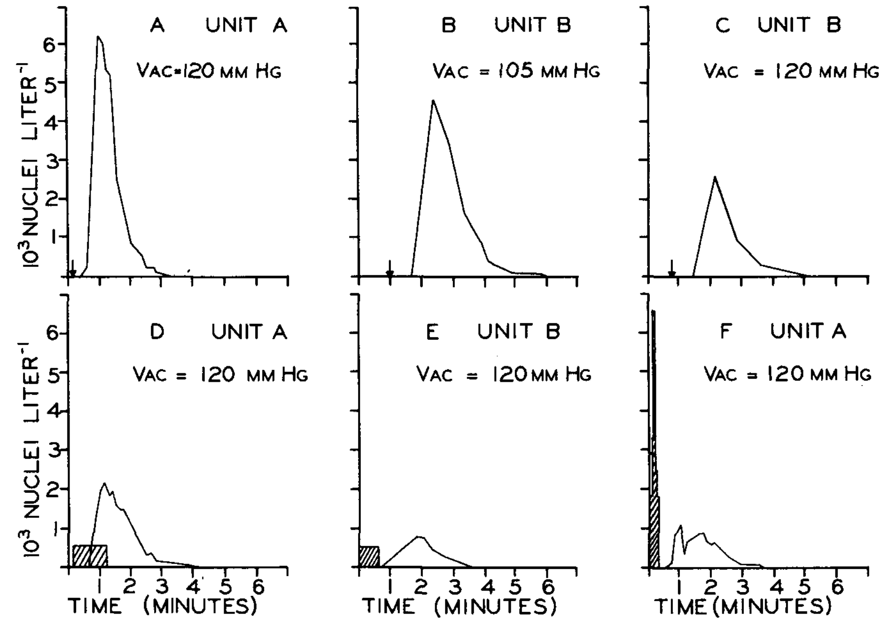

FIG. 4. Responses of two NCAR ice nucleus counters to various input forms. (The arrows show times of "puff" inputs. The hatched areas represent input density functions of $1/I\Delta t_i$.)

the rare event is an ice nucleus not being detected until the Ith time increment. If these rare events are randomly distributed, the variance is equal to the mean number of increments (unitless). The coefficient of dispersion is defined as the ratio of these two (Sokal and Rohlf, 1969) and is unity if the distribution is exactly Poisson. The counter data yielded ratios of variance-to-mean on the order of 10, showing an intense "clumping" (*ibid.*), meaning that there is a tendency for the recorded counts to be grouped over a smaller time span than predicted by the Poisson distribution. This precludes the use of the Poisson assumption in analyses. In addition, the definition of zero time casts uncertainty on such an application.

The instrument-induced standard deviations were found according to (5) using the three types of input outlined previously. Figs. 5 and 6 show that there is less certainty as the peak count decreases. This is expected because the turbulence within the chamber would have its effect more noticeable with a smaller density of ice nuclei. In addition, the turbulence could have some dependence upon the latent heat liberated during phase transition forcing a variability dependent upon the ice nucleus concentration. There appears to be a definitive lower and upper limit to the plots with arithmetic averages showing the induced standard deviation to be on the order of 30–40 s. Estimating the true variance by applying an average to (5) could conceivably give values less than zero; but applications so far have found this to be rare, occurring only during encounters with presumably very thin plumes near to their point source. There is more induced variance for Unit A because the lower two scales had a slow analog output decay rate.

5. Applications

The conversion of the raw data to counts per liter is a straightforward process involving the procedures exemplified in Tables 2 and 3. It is advantageous to have the counts be a function of time rather than distance because it is more convenient to estimate variance contributions in this unit. From (5), the true variance σ_y^2 is estimated and the next step is to reconstruct a distribution based on this parameter.

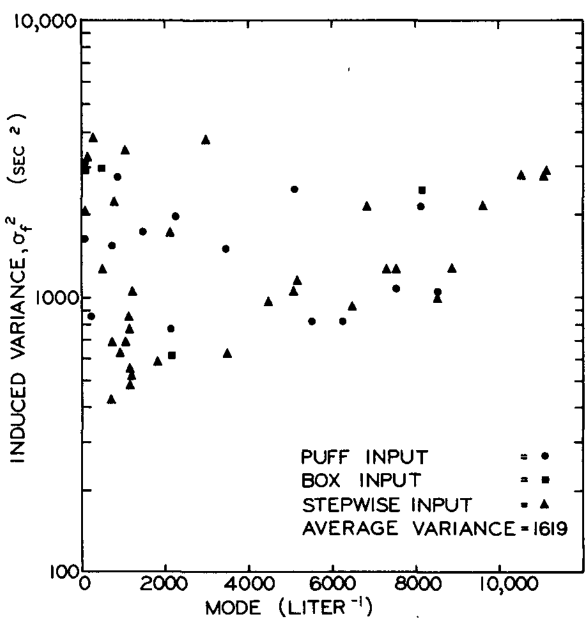

FIG. 5. Instrument induced variance for Unit A.

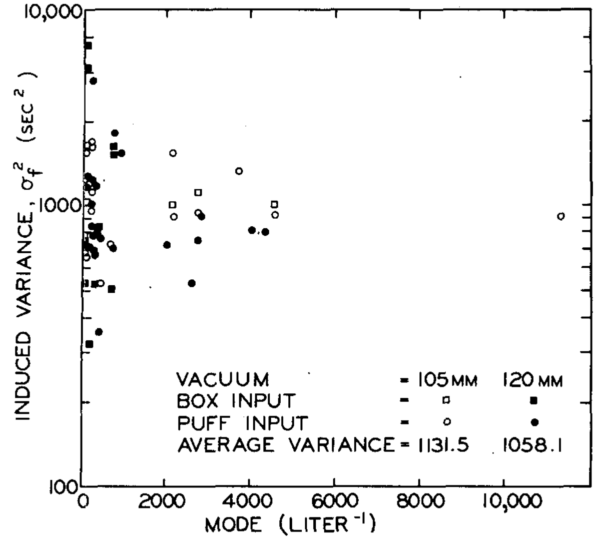

FIG. 6. Instrument induced variance for Unit B.

If the continuous density function is $f(t)$, whose spread is described by σ_y, and the interval of data retrieval is Δt, then the true plume has a time-count density of

$$C_i = N\Delta t f(t), \qquad (9)$$

where N is the total number of counts registered for that pass minus background, or

$$N = \sum_{i=1}^{I} C_i. \qquad (10)$$

The question remains as to specifying $f(t)$. For long averaging times and, presumably, distances, it has been shown theoretically and empirically that diffusion tends to present a Gaussian profile (Sutton, 1953). For this assumption

$$f(t) = \frac{1}{(2\pi)^{\frac{1}{2}}\sigma_y} \exp[-(t-\bar{t})^2/2\sigma_y^2]. \qquad (11)$$

The time where half the total number of counts is encountered (median) rather than the time of mode should be used for $\bar{t}$.

For short downwind distances of 2 km or less from an artificial source of ice nuclei, the plume cannot be assumed to be spread to Gaussian proportions, and a box distribution would seem more appropriate. In this case, σ_y is assumed to be equal to width$/(12)^{\frac{1}{2}}$ and

$$f(t) = \begin{cases} 1/\sigma_y(12)^{\frac{1}{2}}, & |t-\bar{t}| \leqslant \sigma_y(12)^{\frac{1}{2}}/2 \\ 0, & \text{elsewhere}. \end{cases} \qquad (12)$$

If one is only interested in the peak count, the choice between (11) or (12) is not overly critical because the ratio of the peaks is 1.38 in favor of the Gaussian assumption.

From this point, it is a simple process to convert time to distance and incorporate the proper lag time. Once again the lag to median is recommended for positioning the processed plume. If the plume is not reconstructed from a treatment of the variance, the lag to mode would be more appropriate, due to the skewness of the raw response.

Fig. 7 is an example of the treatment of raw data according to the above procedures. Although the variance of the processed profile is smaller, there is a smoothing effect to the raw counts, and it is not uncommon to have the unadjusted peak count be larger. The large fluctuations of the raw counts are responsible for this.

6. Conclusions

The techniques outlined above provide a means to remove some of the uncertainty in interpreting data provided by aircraft-mounted ice nucleus counters. In parameterizing the responses of two NCAR ice nucleus counters it has been shown that there is a great deal of scatter which is due, primarily, to the large size of the cloud chambers of the units and the lack of homogeneity within. There is less scatter among the individual parameters as the peak values increase, reinforcing this view. Another factor which greatly influences the response characteristics is the size of the inlet to the cloud chamber. On a third unit there was a smaller orifice which directed the sampled volume too quickly through the chamber

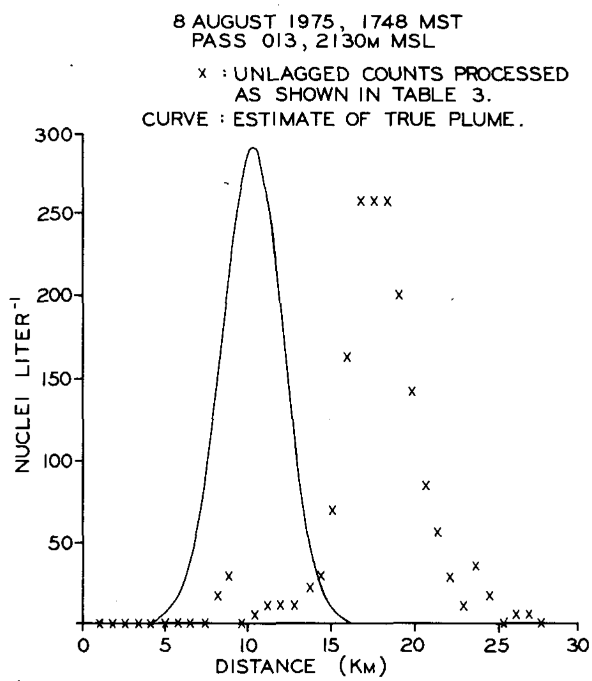

FIG. 7. Example of raw response and estimate of true response. (Unit B with 120 mm Hg vacuum and downwind distance of 5 km.)

without sufficient mixing. This resulted in very short lag times and counts which were an order of magnitude too low in comparison tests with Unit B. A small baffle at the inlet eliminated this problem. This orifice size is critical to provide a turbulent inlet jet. The minimal size of the opening should be $\frac{5}{8}$ inch for the NCAR counter,[1] whereas it was only $\frac{1}{2}$ inch on this counter.

The authors preferred the integrating analog electronics over the digital because of the smoothness of response of the former. The first scale of the digital (Unit B) had a sampling time of 120 s which was entirely too long for anything other than background sampling of natural ice nuclei. Normally, plume tracing with Unit B was done on higher scales involving sampling times $\leqslant 12$ s. There was also a feature available on Unit B, which would automatically switch scales while unattended. Although this would have good applications in static sampling, it is not recommended for airborne use because of the lower resolution.

The parameters listed should be used as a guide only. Each counter will have its own response characteristics and each must be carefully calibrated. The techniques described above are not limited to the NCAR counters. Acoustical detection requires a long growth time and hence the lags and induced variances can be expected to be large. On the other hand, the Mee type counter should have smaller lags and variances, because smaller crystals can be detected optically, requiring a shorter growth period, and a smaller cloud chamber is possible.

Acknowledgments. This research was supported by the Montana Power Company and the Interim Weather Modification Board of the Alberta Hail Project through I. P. Krick Associates of Canada, Ltd. Gerhard Langer of NCAR is gratefully acknowledged for his conscientious and substantial assistance in both projects.

APPENDIX

List of Symbols

- C_i recorded count at data interval i (time^{-1} or liter^{-1})
- $f(t)$ density function (time^{-1})
- I number of samples; also, number of box inputs in an approximation of a normal distribution
- k_i true spread of particles about the mean (time or distance)
- N total count over one sample run (dimensionless)
- t_i time of known sample input
- $\bar{y}$ mean position of plume in time or space for sample run (time or distance)
- Δt_i time interval
- ϵ_{ij} false or instrument-induced spread of jth particle about $(\bar{y}+k_i)$ (time or distance)
- σ_c^2 total or indicated variance (time^2 or distance^2)
- σ_y^2 true variance of sampled plume (time^2 or distance^2)
- σ_f^2 variance induced by instrument (time^2 or distance^2)

[1] Personal communication with G. Langer.

REFERENCES

Fukuta, N., and G. K. Kramer, 1968: A fast activation continuous ice nuclei counter. *J. Rech. Atmos.*, **3**, 169–173.

Langer, G., 1973: Evaluation of NCAR ice nucleus counter. Part I: Basic operation. *J. Appl. Meteor.*, **12**, 1000–1011.

——, J. Rosinski and C. Edwards, 1967: A continuous ice nucleus counter and its application to tracking in the troposphere. *J. Appl. Meteor.*, **6**, 114–125.

Mood, A. M., and F. A. Graybill, 1963: *Introduction to the Theory of Statistics*. McGraw-Hill, 443 pp.

Rottner, D., S. R. Brown and O. H. Foehner, 1975: The effect of persistance of AgI on randomized weather modification experiments. *J. Appl. Meteor.*, **14**, 939–945.

Sokal, R. R., and F. J. Rohlf, 1969: *Biometry*. W. H. Freeman and Co., 776 pp.

Super, A. B., 1974: Silver iodide plume characteristics over the Bridger Mountain Range, Montana. *J. Appl. Meteor.*, **13**, 62–70.

——, C. A. Grainger, J. T. McPartland, V. L. Mitchell and R. H. Yaw, 1972: Atmospheric water resources management program, Final Report-Part I. Bureau of Reclamation Contract No. 14-06-D-6798, Montana State University, Bozeman, 425 pp.

——, J. T. McPartland and J. A. Heimbach, Jr., 1975: Field observations of the persistence of AgI-NH$_4$I-acetone. *J. Appl. Meteor.*, **14**, 1572–1577.

Sutton, O. G., 1953: *Micrometeorology*. McGraw-Hill, 333 pp.

Turner, F. M., and L. F. Radke, 1973: The design and evaluation of an airborne optical ice particle counter. *J. Appl. Meteor.*, **12**, 1309–1318.